Biochimica et Biophysica Acta, 1059 (1991) 76–90

ADONIS 000527289100181F

BBABIO 43439

Stark effect spectroscopy of carotenoids in photosynthetic antenna and reaction center complexes

David S. Gottfried, Martin A. Steffen and Steven G. Boxer

Department of Chemistry, Stanford University, Stanford, CA (U.S.A.)

(Received 10 December 1990)

Key words: Stark effect; Electric field effect; Carotenoid; Carotenoid bandshift

The effects of electric fields on the absorption spectra of the carotenoids spheroidene and spheroidenone in photosynthetic antenna and reaction center complexes (wild-type and several mutants) from purple non-sulfur bacteria are compared with those for the isolated pigments in organic glasses. In general, the field effects are substantially larger for the carotenoid in the protein complexes than for the extracted pigments and larger for spheroidenone than spheroidene. Furthermore, the electrochromic effects for carotenoids in all complexes are much larger than those for the Q_x transitions of the bacteriochlorophyll and bacteriopheophytin pigments which absorb in the 450–700 nm spectral region. The underlying mechanism responsible for the Stark effect spectra in the complexes is found to be dominated by a change in permanent dipole moment of the carotenoid upon excitation. The magnitude of this dipole moment change is found to be considerably larger in the B800-850 complex compared to the reaction center for spheroidene; it is approximately equivalent in the two complexes for spheroidenone. These results are discussed in terms of the effects of differences in the carotenoid functional groups, isomers and perturbations on the electronic structure from interactions with the organized environment in the proteins. These data provide a quantitative basis for the analysis of carotenoid bandshifts which are used to measure transmembrane potential, and they highlight some of the pitfalls in making such measurements on complex membranes containing multiple populations of carotenoids. The results for spheroidenone should be useful for studies of mutant proteins, since mutant strains are often grown semi-aerobically to minimize reversion.

Introduction

Carotenoids are widely distributed in nature and serve a wide range of functions [1]. They are especially important in photosynthetic systems, where they serve the dual functions of light harvesting and photoprotection [2]. In addition to these important physiological roles, shifts in the absorption spectra of carotenoids have been widely used to measure transmembrane potentials and the electrogenicity of charge separation steps [3]. Underlying the utility of these band shifts is quantitative information on the change in dipole moment, $\Delta\mu_A$, and polarizability, $\Delta\alpha$, for these chromophores in the protein environment. During the past few years, our laboratory and others have investigated the effects of applied electric fields (Stark effect spectroscopy or electrochromism) on the absorption [4–7] and emission [8,9] spectra of photosynthetic reaction center (RC) complexes; Stark effect data for the bacteriochlorophyll *a* (BChl *a*) Q_y region of antenna complexes is presented in an accompanying paper [10]. In the course of these studies we examined the Q_x region of the Stark effect spectrum for the R26 carotenoidless mutant of *Rb. sphaeroides* [4,5] and found only weak electrochromic effects. In the following we demonstrate that, when carotenoids are present in the protein complexes, much larger effects are observed in this spectral region, and these can be attributed to the carotenoid chromophores. Even larger effects are observed in antenna complexes. A preliminary report focusing exclusively on spheroidene in the B800-850 antenna complex has been presented else-

Abbreviations: BChl, bacteriochlorophyll; LDS, lithium dodecyl sulfate; PVA, poly(vinyl alcohol); PMMA, poly(methyl methacrylate); 3MP, 3-methylpentane.

Correspondence: S.G. Boxer, Department of Chemistry, Stanford University, Stanford, CA 94305, U.S.A.

where [11]; here we compare those results with a complete set of data on two different carotenoids in antennas and both wild-type and mutant reaction centers.

The B800-850 (LHII) antenna complex from purple non-sulfur bacteria such as *Rb. sphaeroides* has been characterized in detail with respect to composition [12,13], electronic absorption and emission spectroscopy [14], Stark effect spectroscopy in the BChl *a* Q_y region [10], and energy transfer [15]. Diffraction quality crystals of B800-850 from different bacteria have been prepared by several groups [16–18], but a structure is not yet available. It is generally agreed that the complex consists of BChl *a* and carotenoid chromophores in a 2:1 ratio [13] which are complexed with a pair of α-helical transmembrane polypeptides [19]. In the model of Kramer et al. [14], the antenna is a repeat of minimal units containing six BChl *a*, three carotenoids and two each of the α and β proteins. The function of the carotenoids is both to transfer energy to the lower-energy BChl *a* components [15] and to quench potentially reactive and destructive BChl *a* triplet states, should they be formed [2].

A single carotenoid molecule is also present in the reaction center complex. Its location and approximate structure have been determined in *Rps. viridis* [20] (the carotenoid is 1,2-dihydroneurosporene) and *Rb. sphaeroides* [21,22]; however, in both cases the structural data are less than ideal due to disorder. In both species the carotenoid is located adjacent to the monomer BChl on the M-side (light-driven electron transfer proceeds down the L-side). As in the antenna complexes, the carotenoid functions both to harvest excitation energy and to quench unwanted triplet states [2]. A detailed mechanism for the quenching of the special pair triplet state has been proposed based upon measured triplet energies [23,24], energy transfer rates [25], and pigment modification experiments [26].

The chemical composition of the carotenoids present in RCs and antennas from *Rb. sphaeroides* depends on the growth conditions: under anaerobic growth conditions, the dominant carotenoid is spheroidene, while under semi-aerobic growth conditions a component of spheroidenone accumulates with the exact fraction present dependent on the level of O_2 during cell growth [27]. In *Rb. sphaeroides* cells which are grown anaerobically, the major carotenoid (> 95%) is spheroidene, while in cells that are grown in the presence of oxygen, spheroidenone accounts for about 80% of the carotenoid in RCs and about 30% in the B800-850 complex [27], the remainder being spheroidene. The carotenoids in the B800-850 complex are all-*trans* [28], and their transition dipole moments, which are roughly parallel to the long molecular axis, lie approx. 45–50° away from the plane of the membrane [29]. In the RC from *Rb. sphaeroides*, the

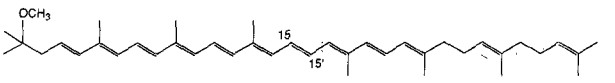

SPHEROIDENE

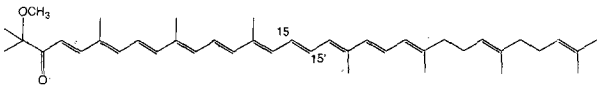

SPHEROIDENONE

carotenoid is believed to be present as the 15-15′-*cis* isomer, with slight deviations from planarity near the ends of the molecule [30,31].

For most of the recent work with *Rb. sphaeroides* and *Rb. capsulatus* mutant and pseudo-wild-type RCs, cells have been grown non-photosynthetically to minimize the possibility of reversion, so that a large fraction of the carotenoid is spheroidenone. To date, strains deficient in carotenoid biosynthesis analogous to the *Rb. sphaeroides* R26 strain have not been used to produce RC or antenna mutants. Because the relative amounts of the two carotenoids are very sensitive to growth conditions, and because most laboratories are not growing mutants under strictly controlled oxygen partial pressure, there is a high level of variability in the ratio of spheroidene to spheroidenone among individual preparations. Since the two carotenoids have different sensitivities to an applied electric field, vide infra, it is important to investigate field effects on both.

Stark effect spectroscopy can provide direct information on the change in dipole moment, $\Delta\boldsymbol{\mu}_A$, between the ground and excited state, on changes in polarizability, $\Delta\boldsymbol{\alpha}$, and on field dependent changes in oscillator strength (due to transition polarizability and hyperpolarizability). If these effects are independent, then upon application of an external electric field to an immobilized isotropic sample, changes in dipole moment lead to band broadening (second derivative-shaped features in the Stark effect spectrum), changes in polarizability lead to band shifts (first derivative effects), and changes in oscillator strength produce zeroth and first derivative effects. For isotropic samples, the magnitude of the effects due to both $\Delta\boldsymbol{\mu}_A$ and $\Delta\boldsymbol{\alpha}$ have a quadratic dependence on external field as long as the Stark splitting is less than the inhomogeneous linewidth. One of the first applications of this method to a molecule from a biological sample was a measurement of $\Delta\boldsymbol{\mu}_A$ for retinal in bacteriorhodopsin [32]. In that case, a very large change in dipole moment was observed, $|\Delta\boldsymbol{\mu}_A| = 13$ Debye. Retinal, especially upon formation of a protonated Schiff's base linkage to the protein, is a very unsymmetric molecule, so large ground and excited state permanent dipole moments

are reasonable. More symmetric polyenes with 2–5 conjugated double bonds have also been studied in organic solvents [33,34], and relatively small values of $\Delta\mu_A$ (1–4 D) and relatively large changes of $\Delta\alpha$ were observed as expected. Based on these results, we expected that the relatively symmetric carotenoids found in photosynthetic assemblies would not exhibit large Stark effects attributable to $\Delta\mu_A$; however, as described in the following, the effects are often substantially larger than for retinal and are always larger than for any of the bacteriochlorophyll or bacteriopheophytin pigments.

Materials and Methods

The B800-850 complex from *Rb. sphaeroides* (wild-type strain 2.4.1) grown anaerobically and pure spheroidene were kindly provided by Carol Violette in Prof. Frank's laboratory (University of Connecticut). The B800-850 complex and RCs from *Rb. sphaeroides* (wild-type strain WS 231) grown semi-aerobically were purified as described elsewhere [10,35]. Treatment of the B800-850 complex with lithium dodecyl sulfate (LDS) for attenuation of the 800 nm band followed literature methods [36]; data for the BChl *a* Q_y region are reported in the accompanying paper [10]. Spheroidenone was extracted from semi-aerobically grown cells and purified as described in Ref. 13. The chemical purity of both extracted carotenoids was ascertained by HPLC analysis using a non-endcapped Zorbax ODS column [37]. Reconstitution of spheroidene and spheroidenone into RCs of the *Rb. sphaeroides* R26 carotenoidless mutant was performed as described in [26].

Absorption and Stark effect spectra of protein samples were measured in glycerol/buffer glasses (1 : 1, v/v) at 77 K [10]. One exception was the LDS-treated B800-850 complex, which was embedded in films of poly(vinyl alcohol) (PVA) [4,10] *. The extracted carotenoids were studied in 3-methylpentane (3MP) glasses or embedded in poly(methyl methacrylate) (PMMA) films [5]. The apparatus for electric field effect measurements and the determination of ζ_A, the angle between $\Delta\mu_A$ and the transition moment, have been previously described [4,5,10]. Because different bands can, in principle, have different values of ζ_A, Stark effect measurements are made at the magic angle, $\chi = 54.7°$, where χ is the angle between the electric polarization of the probing light and $\mathbf{F}_{ext}$. At the magic angle, ΔA is independent of ζ_A. The magnitudes of ΔA for all systems studied were found to scale quadratically with the externally applied electric field as expected for an isotropic sample, and the spectra shown in the figures have been scaled to the same applied field for ease of comparison. The actual electric field felt by a chromophore due to the externally applied field, $\mathbf{F}_{ext}$, is denoted $\mathbf{F}_{int}$, where $\mathbf{F}_{int} = f \cdot \mathbf{F}_{ext}$ and f is the local field correction factor. An ellipsoidal cavity approximation has been shown to be appropriate for linear polyenes [38]. Since the difference dipole moment is expected and found to lie along the long axis of the molecule, vide infra, the major axis component of the local field correction tensor, often denoted f_x, is relevant. For typical ellipsoidal cavity parameters of polyenes and solvent dielectric constants, f_x is between 1.0 and 1.1 [33]. Values of $|\Delta\mu_A|$ are reported in units of Debye/f to facilitate comparison, and the subscript x is dropped for simplicity. When no external field is applied, i.e., $\mathbf{F}_{ext} = 0$, then $\mathbf{F}_{int} = 0$; however, this does not mean that an internal electric field due to the matrix is absent. There are still contributions to the matrix field due to the potentials felt by the chromophore in its local environment, and, as discussed below, these internal matrix fields can be quite large (typically larger than $\mathbf{F}_{ext}$) and have a well-defined magnitude and spatial relationship to the chromophore in the organized environment of the protein. We note that the internal matrix field and the local field correction factor are separate physical quantities.

The first and second derivatives of the absorption spectra were obtained either directly from the data (generally smoothed using a Savitsky-Golay moving window or Fourier filtering) or by fitting the data to a combination of skewed Gaussian bands, followed by numerical differentiation. Contributions of zeroth, first, and second derivatives to the observed Stark effect spectrum (the ΔA spectrum) were then determined by a least-squares fit to the expected dependence [39,40]. Although this classical method introduced by Liptay and co-workers [39] is often successful, we have measured the Stark spectra of many complex systems which appear to deviate from a simple sum of derivatives. Possible explanations for this behavior are discussed by Reimers and Hush [41] and Wortmann et al. [42]; our approach to the data analysis in such cases is described in detail below.

Results

B800-850 complex

The absorption, Stark effect, and second derivative of absorption in the carotenoid and BChl *a* Q_x region

* In the course of these investigations we discovered that the Stark effect spectra of frozen glass samples containing ionic detergents such as LDS or SDS are completely dominated by large oscillations. The origin of these interesting oscillations is not known and is being investigated. No such oscillations are observed in frozen glasses containing non-ionic detergents such as LDAO, and they are not observed when samples containing ionic detergents are embedded in PVA films. For this reason PVA films were used to compare native and LDS-treated samples.

for the B800-850 antenna complex isolated from anaerobically grown (spheroidene-containing) [12] and semi-aerobically grown (spheroidene/spheroidenone) *Rb. sphaeroides,* are shown in Figs. 1 and 2, respectively. The Stark effect spectra are compared with each other in Fig. 3. The electric field induced change in the absorption of the origin and vibronic bands of the carotenoid is huge (about 100-times larger) compared to that measured for the Q_x transitions of the BChl *a* chromophores around 600 nm. The absorption spectrum of spheroidene in the complex (Fig. 1A) shows a well-resolved series of vibronic bands, and a prominent, second-derivative-shaped Stark effect feature is observed for each band, including all of the shoulders on the bands. The angle ζ_A between $\Delta\mu_A$ and the transition dipole moment was found to be $\zeta_A = 10 \pm 2°$ and is the same for each vibronic component. Because of the excellent resolution of bands in the absorption spectrum of the spheroidene-containing B800-850 complex and the close agreement of the Stark effect with the second derivative of the absorption, an accurate value $|\Delta\mu_A| = (15.3 \pm 0.7)$ D/*f* is determined, and little, if any, contribution due to a change in polarizability is observed (no first-derivative lineshape). Within the experimental uncertainty, this same value of $|\Delta\mu_A|$ is obtained for each vibronic component.

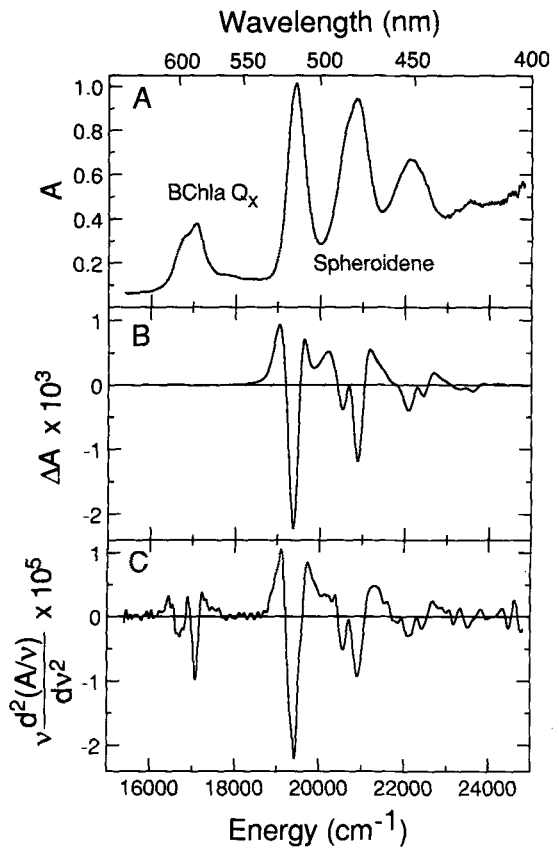

Fig. 1. (A) Absorption, (B) Stark effect and (C) second derivative of absorption spectra of the B800-850 complex obtained from *Rb. sphaeroides* wild-type strain 2.4.1 grown under anaerobic conditions (spheroidene is the carotenoid). $T = 77$ K, $F_{ext} = 10^5$ V/cm and the ΔA spectrum is shown for $\chi = 54.7°$

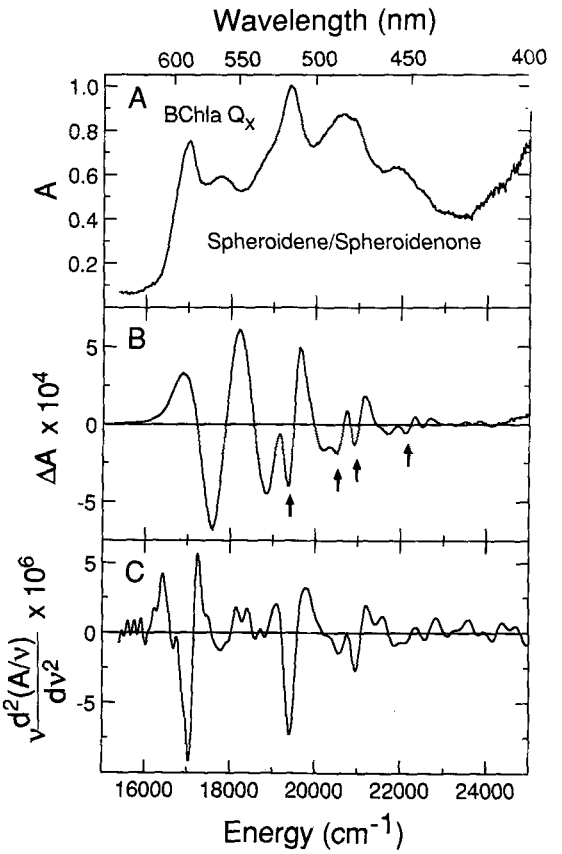

Fig. 2. (A) Absorption, (B) Stark effect and (C) second derivative of absorption spectra of the B800-85 complex obtained from *Rb. sphaeroides* wild-type strain WS 231 grown under semi-aerobic conditions (spheroidenone and spheroidene present). Features due to spheroidene are marked with arrows based on a comparison with data in Fig. 1 (cf. Fig. 3). $T = 77$ K, $F_{ext} = 10^5$ V/cm and the ΔA spectrum is shown for $\chi = 54.7°$.

Semi-aerobically grown B800-850 complex contains a mixture of the two carotenoids with an approximate composition of 70% spheroidene and 30% spheroidenone [27]. Although the absorption spectrum in the carotenoid region (Fig. 2A) is less well resolved due to the overlap of features from the two types of carotneoid and the intrinsically more congested spectrum of spheroidenone (see below), the Stark effect spectrum shows a surprisingly clear progression of very large features (Fig. 2B). The component of spheroidene which is present is clearly evident in the Stark effect spectrum at exactly the same energies as in Fig. 1 (highlighted with arrows in Fig. 2B); this is most clearly seen in Fig. 3. Thus, the contribution from spheroidenone is associated with the Stark effect bands at 17575, 18818 and 20175 cm^{-1}. Qualitatively, the Stark effect for these features is at least as large as for the spheroidene component. The poorer resolution in the absorption spectrum and overlap with features due to

spheroidene makes it much more difficult to quantitatively analyze the data further, and this is deferred to the Discussion section.

Samples of the B800-850 complex containing spheroidene were also examined in PVA films (Fig. 4) and give essentially the same qualitative and quantitative observations as the glass sample shown in Fig. 1. The Stark spectrum has mainly second-derivative contributions to the lineshape with $|\Delta\mu_A| = (13 \pm 3)$ D/f and $\zeta_A \approx 0°$. Spectral overlap due to the slightly increased linewidths in PVA compared to the glycerol/buffer glass makes a more quantitative analysis problematic, but it also appears that some of the vibronic bands have values of $|\Delta\mu_A|$ that are different from those for the origin band. Related issues have been raised in model calculations and experimental measurements of the electro-optic spectrum of a symmetric linear polyene [42], and these will be discussed further below. LDS-treated samples of the antenna complex in PVA (Fig. 4) give strikingly different results than samples solubilized with LDAO *. The Stark spectrum can be seen to contain a significantly larger component of first-derivative lineshape and the overall magnitude of the effect (for a given absorption and applied field) is much smaller (cf. Fig. 1). Fitting of the angle-dependent spectra to a sum of derivatives results in $|\Delta\mu_A| = (6 \pm 1)$ D/f, $\zeta_A < 20°$, and a large polarizability change ($|\mathrm{Tr}(\Delta\alpha)| \approx 1000$ Å$^3/f^2$), although here it is evident that $|\Delta\mu_A|$ and $\Delta\alpha$ are variable for the different vibronic and/or population components.

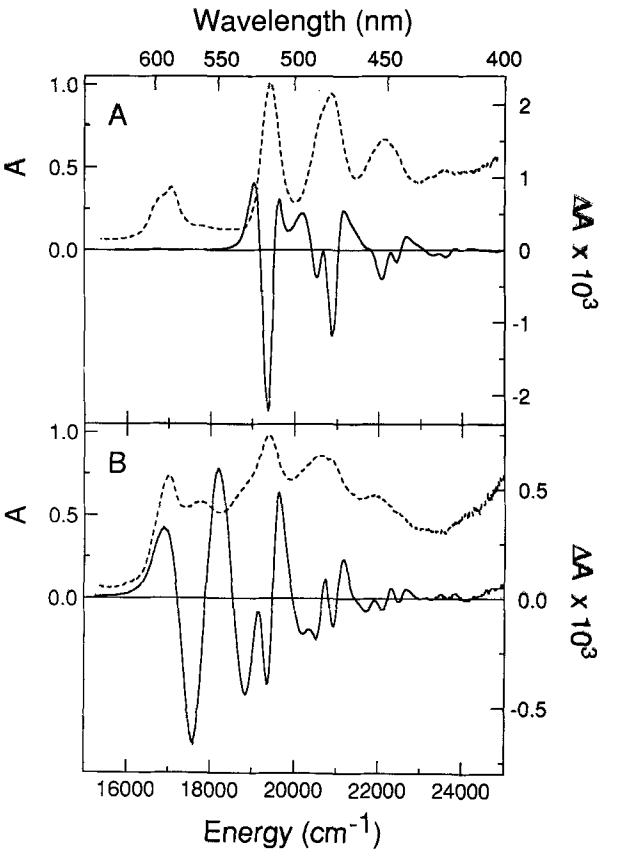

Fig. 3. Comparison of absorption (– – –, left ordinate) and Stark effect (———, right ordinate) spectra for the B800-850 complex containing (A) spheroidene (Fig. 1), and (B) a mixture of spheroidene and spheroidenone (Fig. 2).

Reaction center complexes

RCs from the carotenoidless R26 mutant of *Rb. sphaeroides* were reconstituted with pure spheroidene and spheroidenone in order to obtain the cleanest possible Stark effect data for these carotenoids in the RC (this was not an option with the B800-850 complex complex as no reconstitution procedure is presently available). Relative to the B800-850 complex (cf. Fig. 1), the Stark effect for spheroidene is much smaller in the RC complex (Fig. 5, note the vertical scale of the ΔA spectrum). Variation in the lineshape of ΔA as a function of the experimental angle χ (see Fig. 5B) indicates that there is substantial overlap among the spheroidene peaks and with the Q_x and Soret bands of the BChl and BPheo. The Stark effect spectrum is a mixture of second and first derivative effects, but due to the presence of other absorption peaks, the data cannot be reliably fit to extract $|\Delta\mu_A|$ and $\Delta\alpha$. Assuming only a second-derivative contribution to the Stark effect, we can approximate $|\Delta\mu_A| = 3$–8 D/f (depending on wavelength).

Data obtained for *Rb. sphaeroides* R26 RCs reconstituted with pure spheroidenone and several semi-aerobically grown wild-type and mutant RCs are shown in Fig. 6. As for the B800-850 complex, the carotenoid vibronic bands are not well resolved in the absorption spectra. However, all the Stark effect spectra show a regular progression of bands whose separation is about 1350 cm^{-1}. This separation is also very similar to that found for the spheroidenone component in the B800-850 complex (Fig. 2). The magnitude of ΔA in this region is comparable to that in the B800-850 complex for samples of comparable concentration at comparable external fields. Furthermore, in contrast to the B800-850 complex from the same organism grown under the same conditions (Fig. 2), the contribution from spheroidene is not evident in the RC ΔA spectrum. This observation is consistent with the notion that the absorption of spheroidenone in the RC is much more sensitive to an applied field than spheroidene (Fig. 6). It is also possible that the RC binds spheroidenone somewhat better than spheroidene [27], and consequently is enriched in the former compared to the B800-850 complex. Qualitatively, as seen in Fig. 6, nearly identical results were obtained in the carotenoid

* See previous footnote, p. 78.

region for RCs isolated from *Rb. capsulatus* wild-type and heterodimer strains [43], and for *Rb. sphaeroides* wild-type, heterodimer [35] and reverse heterodimer [44] strains, all grown semi-aerobically. In order to facilitate comparison, the absorption spectra in Fig. 6 were scaled so that the optical absorbance of the BChl *a* monomer Q_y band near 800 nm is 1, and the Stark effect spectra were scaled to an applied field of 10^5 V/cm. As in the B800-850 complex, the poor resolution of the absorption spectrum makes a quantitative analysis of the contributions of various derivatives to the total ΔA problematic for spheroidenone-containing RCs (see Discussion).

Pure carotenoids in organic glasses

In order to help distinguish the intrinsic properties of the chromophores from effects induced by the various protein matrices, the Stark effect spectra for pure spheroidene and spheroidenone were examined in a non-polar glass (3MP) and a polymer film (PMMA). The results for PMMA films are shown in Figs. 7 and 8 for spheroidene and spheroidenone, respectively, and are compared with the first and second derivatives of the absorption spectra. For spheroidene, the ΔA spectrum has nearly the same shape as the first derivative except that it is shifted approx. 250 cm^{-1} to lower energy. The data (origin and all vibronic bands) can also be fit quite well by a sum of first derivative and second derivative contributions. This provides an upper limit for the value of $|\Delta\mu_A| \leqslant 4.7\ D/f$ and a lower limit for $|\mathrm{Tr}(\Delta\alpha)| \geqslant 500\ Å^3/f^2$. The angle ζ_A between $\Delta\mu_A$ and the transition moment is $15 \pm 2°$, and the long axis of the polarizability tensor was also found to be approximately parallel to the transition moment direction. Within the sensitivity of the measurement, identical results are obtained for spheroidene in a 3MP glass (data not shown) and a PMMA film.

For spheroidenone, the ΔA spectrum closely resembles the absorption second-derivative spectrum, except that the Stark effect bands are shifted about 150 cm^{-1} and about 330 cm^{-1} to the red in PMMA and 3MP, respectively (Figs. 8 and 9). The vibronic components

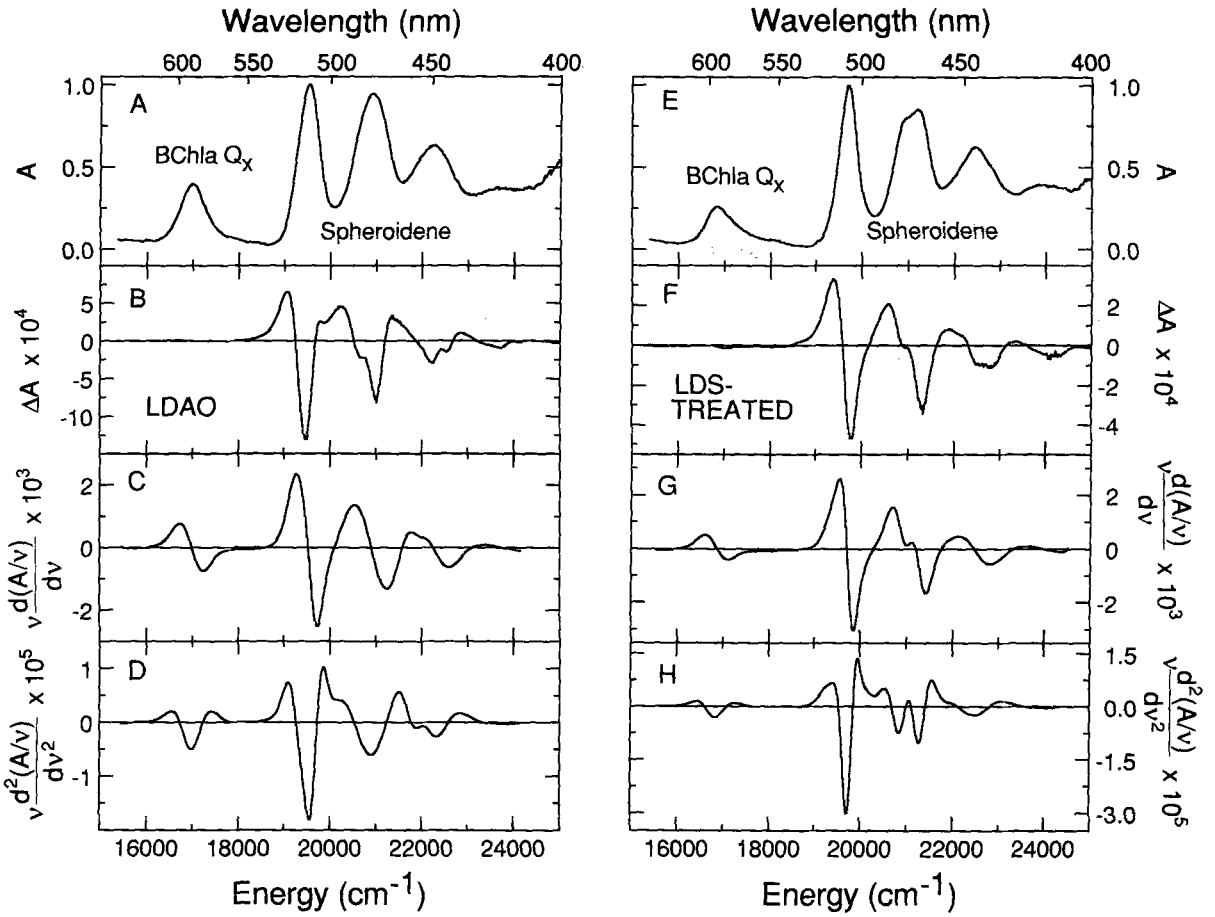

Fig. 4. (A) Absorption, (B) Stark effect, (C) first derivative and (D) second derivative of absorption spectra of spheroidene-containing B800-850 complex solubilized in LDAO and embedded in a PVA film. (E) Absorption, (F) Stark effect, (G) first derivative and (H) second derivative of absorption spectra of spheroidene-containing B800-850 complex treated with LDS and embedded in a PVA film. $T = 77$ K, $F_{ext} = 10^5$ V/cm and the ΔA spectra are shown for $\chi = 54.7°$.

are regularly spaced at about 1400 cm^{-1}, which is similar to that found for isolated spheroidene. There is more overlap of the individual Stark features in spheroidenone samples, and the features are larger than those of spheroidene for a comparable absorption and applied electric field. For the origin band in both matrices, $|\Delta\mu_A| = (20 \pm 2)\ D/f$, and $\zeta_A = 18 \pm 4°$. The vibronic components shown in Figs. 8 and 9 exhibit some variation with respect to both $|\Delta\mu_A|$ and the angle dependence of ΔA, although no trend is obvious. Average values of the molecular parameters for the different vibronic bands in both matrices are $|\Delta\mu_A| = (20 \pm 10)\ D/f$, and $\zeta_A < 22°$.

A summary of the results for the two carotenoids in the various matrices is presented in Table I. Further discussion of the methods used to estimate the values listed when the ΔA spectra are not simply related to derivatives of the absorption spectrum follows below.

Discussion

General principles

It is evident from a cursory examination of the data that the electric field effects on the carotenoid absorption bands in the protein complexes are large, and the lineshapes are generally dominated by contributions which resemble the second derivative of the absorption spectrum, indicative of large apparent values of $|\Delta\mu_A|$. This is a surprising result, as the conjugated π-system in spheroidene is very symmetric. The conjugated carbonyl group in spheroidenone makes its extended π-system considerably less symmetric. It is well known that linear extended π-systems have highly polarizable ground and excited states, with typical values on the order of 100 Å^3 and 500 Å^3 or larger, respectively [34,39]. This contrasts with the case of aromatic π-systems, such as the porphyrins, chlorins and bacteriochlorins, where both the ground and excited state polarizabilities are typically on the order of 50 Å^3. For example, the Stark effect spectrum of BChl *a* Q_y transition resembles closely the second derivative of the absorption spectrum with little first derivative contribution [5].

The lineshape of the Stark effect spectrum for an immobilized isotropic sample of an inversion-symmetric polyene in the absence of solvent (a hypothetical immobilized gas) is expected to be entirely first derivative due to the large polarizability change. An external electric field induces a dipole moment parallel to the direction of $\mathbf{F}_{ext}$, consequently, the Stark effect spectrum is similar in lineshape to that observed for a uniaxially oriented sample (the magnitude of ΔA would be smaller, since all orientations are present). If the molecule is placed in an isotropic solvent and is immobilized, then each molecule experiences an electric field due to the matrix which depends on the particular

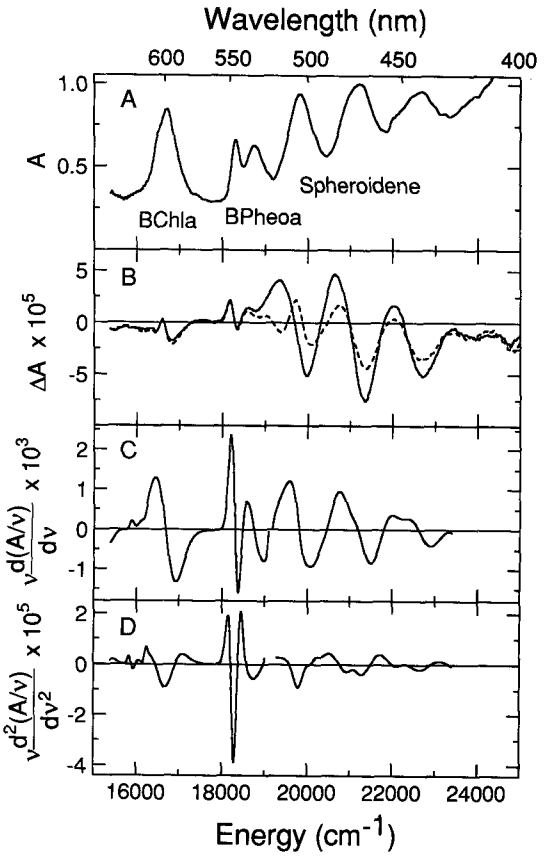

Fig. 5. (A) Absorption, (B) Stark effect, (C) first derivative and (D) second derivative of absorption spectra of reaction centers from *Rb. sphaeroides* R26 mutant reconstituted with spheroidene [26]. $T = 77$ K, $\mathbf{F}_{ext} = 10^5$ V/cm and the ΔA spectra are shown for $\chi = 90.0°$ (– – –) and 54.7° (———).

configuration of solvent molecules in the vicinity of the chromophore, and each such matrix field will induce a dipole moment by interaction with the polarizability tensor. Because the polarizabilities are so large for polyenes, such induced dipole moments can be quite large. It is expected that the range of values of the matrix field will be greatest for the most polar solvents. This effect, often called solvent-induced symmetry breaking, is well documented in the chemical physics literature [34]. If the Stark effect spectrum due to an externally applied field is measured for such a sample, the second derivative-shaped contribution will be determined by the magnitude of the induced dipole moment difference (the induced dipoles are randomly oriented relative to $\mathbf{F}_{ext}$ because both the solvent which induces the dipoles and the solute orientation relative to $\mathbf{F}_{ext}$ are random). A first-derivative lineshape contribution is also expected because of the interaction of the molecular polarizability difference with the external field. If the dipole moment difference induced by the matrix field is very large, then the Stark effect lineshape will be dominated by the second-derivative contribution, even though the first-derivative contribu-

tion due to the interaction of the external field and the polarizability difference is still present. This analysis assumes that the interaction between the internal field and the polarizability is linear, and that higher-order, non-linear effects, which might change the magnitude of $\Delta\alpha$, are not present. This is a reasonable approximation for internal field strengths which are likely to be present in simple matrices.

The situation in an ordered solvent, such as that found for a chromophore bound with a specific orientation in a protein matrix, is a limiting case. In this case the matrix field due to the solvent (protein) always has approximately the same relationship to the polarizability tensor of the chromophore, and induces dipole moments with the same magnitude and direction for every chromophore. Because the protein-chromophore complexes are isotropic with respect to $\mathbf{F}_{ext}$, the Stark effect spectrum is dominated by a second derivative lineshape. This is likely the basic explanation for the lineshape of the Stark effect spectra observed for these complexes.

The data for *trans*-spheroidene provide a clear-cut example of these effects. Although no information is available for this polyene in the gas phase, it is reasonable to expect that $|\Delta\mu_A|$ is approximately zero because of the symmetry of the π-system. When the chromophore is embedded in a non-polar matrix such as 3MP or PMMA, the Stark effect spectrum shows clear evidence for both first and second derivative contributions to the lineshape (Fig. 7). With the assumption that the matrix electric field from the solvent does not change $|\Delta\alpha|$, the value estimated for $|\Delta\alpha|$ is the true molecular property. The appearance of a second derivative contribution in the Stark effect lineshape is due to a dipole moment difference induced by the matrix field which then interacts with the externally applied field. Within this model, its value is not a molecular property, rather it reflects the magnitude of the interaction between the molecule and its environment. When the same chromophore is in an ordered solvent environment, such as the protein of the B800-850 complex, the internal field can induce a very sub-

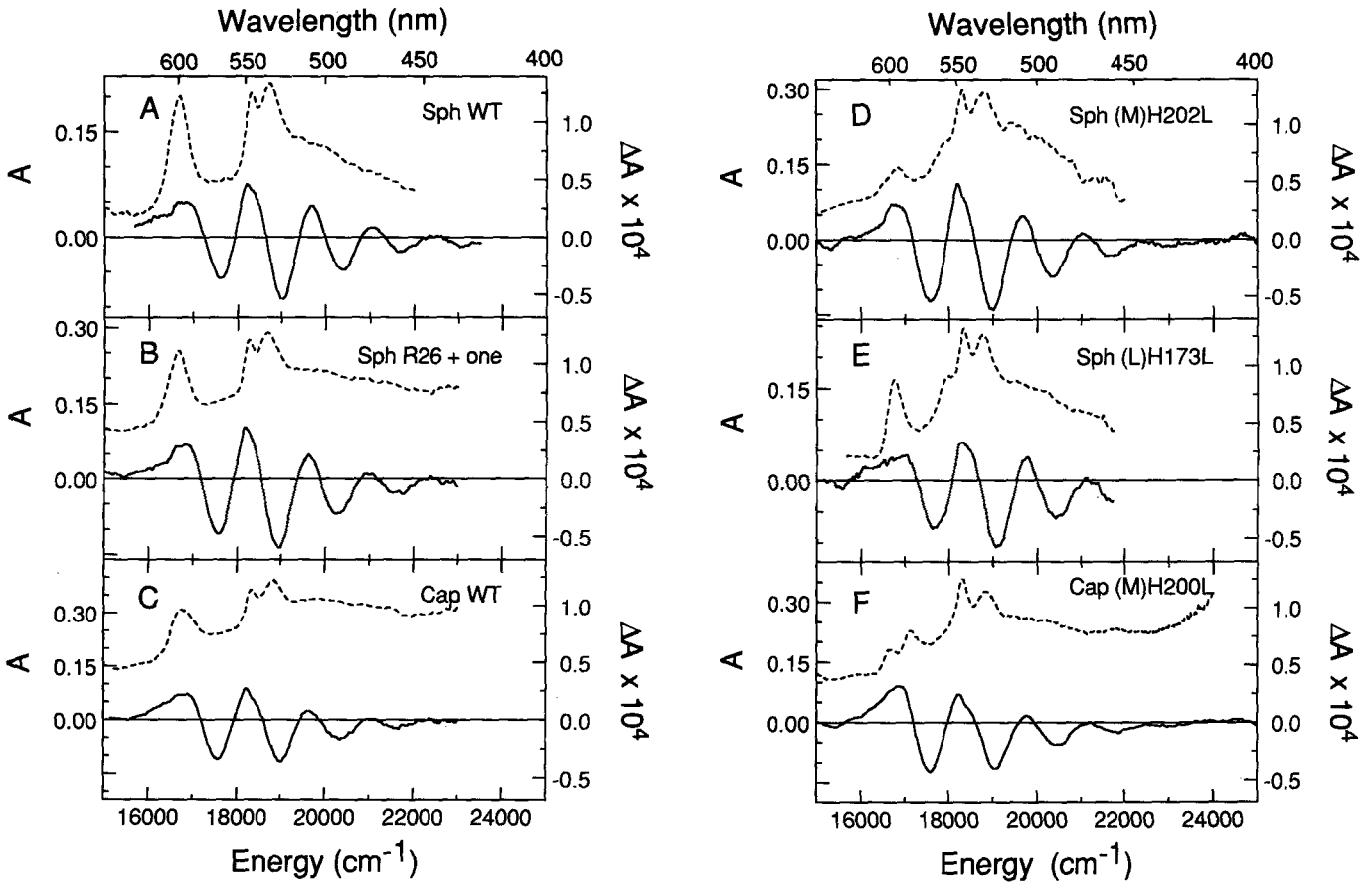

Fig. 6. Comparison of absorption (– – –, left ordinate) and Stark effect (———, right ordinate) spectra for reaction centers containing spheroidenone: (A) semi-aerobically grown *Rb. sphaeroides* wild-type strain WS231, (B) spheroidenone reconstituted into *Rb. sphaeroides* strain R26, (C) semi-aerobically grown *Rb. capsulatus* wild-type, (D) semi-aerobically grown *Rb. sphaeroides* heterodimer mutant (M)H202L, (E) semi-aerobically grown *Rb. sphaeroides* reverse heterodimer mutant (L)H173L, (F) semi-aerobically grown *Rb. capsulatus* heterodimer mutant (M)H200L. $T = 77$ K, $\mathbf{F}_{ext} = 10^5$ V/cm, and the ΔA spectrum is shown for $\chi = 54.7°$. The absorbance of the monomer BChl *a* feature around 800 nm was scaled to 1.0 for all samples to facilitate comparison (see text).

stantial dipole moment, and, for an isotropic distribution of B800-850 complexes with respect to $\mathbf{F}_{ext}$, a pure second derivative lineshape results (Fig. 1). The first-derivative contribution expected from the interaction of the molecular polarizability with the external field should have approximately the same magnitude as in the non-polar solvent. Comparison of the magnitude of the effects in Figs. 1 and 7 suggests that the relative contributions to ΔA from the interaction of the molecular polarizability difference with the external field is somewhat less than that from the interaction of the induced $\Delta\boldsymbol{\mu}_A$, consequently the first-derivative contribution is not observable. If it is assumed that $\Delta\boldsymbol{\alpha}$ of the carotenoid is not different in a polymer matrix and the protein, then the magnitude of the induced difference dipole can be used to estimate the matrix electric field. Using the data for spheroidene in 3MP, and assuming the matrix field is aligned with the long axis of the molecule (the major axis of the difference polarizability tensor), we estimate that a matrix field of greater than $5 \cdot 10^6$ V/cm is present in the carotenoid binding site in the B800-850 complex *.

Further analysis of spheroidene data

The observed electrochromic effect of spheroidene in the B800-850 antenna complex discussed above is the only combination of carotenoid and matrix studied that gives a clearly defined second-derivative-shaped Stark effect resulting in uniform values of the molecular parameters $|\Delta\boldsymbol{\mu}_A|$ and ζ_A for the origin and vibronic bands. This uniformity demonstrates that the effect is essentially due entirely to a change in permanent dipole moment between the ground and excited state, with no discernible contribution from either polarizability, hyperpolarizability, or transition moment changes. Furthermore, there is no evidence that there is any difference in the electronic structure of the three spheroidene molecules in the minimal unit of the antenna complex. This point is made especially clear by comparison of the linewidths of the spheroidene absorption bands in the B800-850 complex and in PMMA

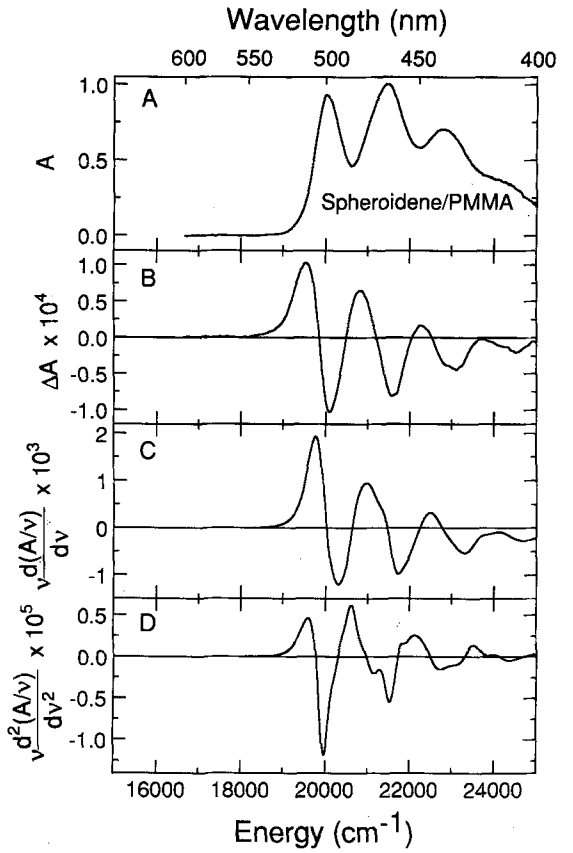

Fig. 7. (A) Absorption, (B) Stark effect, (C) first derivative and (D) second derivative of absorption spectra of pure all-*trans*-spheroidene embedded in a PMMA film. $T = 77$ K, $\mathbf{F}_{ext} = 10^5$ V/cm and the ΔA spectrum is shown for $\chi = 54.7°$.

(Figs. 1 and 7). Given that there are three carotenoids per minimal unit in the antenna complex [14] and different chromophore orientations and positions could lead to differing transition energies, it is striking that the complex shows a narrower lineshape than the chromophore in a PMMA film. This is consistent with a very well structured and similar environment in the vicinity of all three carotenoids.

A comparison of Figs. 1 and 4 reveals that the absorption Stark effect of spheroidene in the B800-850 complex is perturbed only slightly by embedding it in a PVA film, compared to a glycerol/buffer glass. In contrast, samples of B800-850 complex treated with the detergent LDS and embedded in PVA show markedly different behavior. The carotenoid absorption bands in the LDS-treated sample are shifted to higher energy and have lineshapes slightly different from those of the LDAO-solubilized sample (see the second-derivative spectra in Fig. 4). The Stark effect spectrum of the LDS sample shows a large decrease in magnitude and a relatively larger contribution from a first-derivative component compared to that for LDAO. These results are indicative of a profound change in the local environment around the carotenoids in the complex upon LDS treatment, perhaps associated with a major struc-

* The results and analysis may bear on the interpretation of the large Stark effect for the Q_y transition of the dimeric special pair in the RC [4–7]. We and others generally interpret the large value of $|\Delta\boldsymbol{\mu}_A|$ of the special pair relative to that of a monomer BChl as a result of strong coupling to intra-dimer charge-transfer states (this is formally identical to a polarizability [59]). The Stark effects for BChl *a* and BChl *b* are quite well described by second-derivative lineshapes [5], so it appears that $\Delta\boldsymbol{\alpha}$ for these chromophores is quite small. On the other hand, the special pair dimer, with its much larger π system, may be more polarizable than its monomeric constituents. Thus, the environment of the special pair could induce the large value of $|\Delta\boldsymbol{\mu}_A|$; this could also be the case for some of the antenna complexes described in the accompanying paper [10]. The ΔA lineshape for the special pair Q_y transition is quite complex at 2 K and is discussed in detail elsewhere [59,60,62].

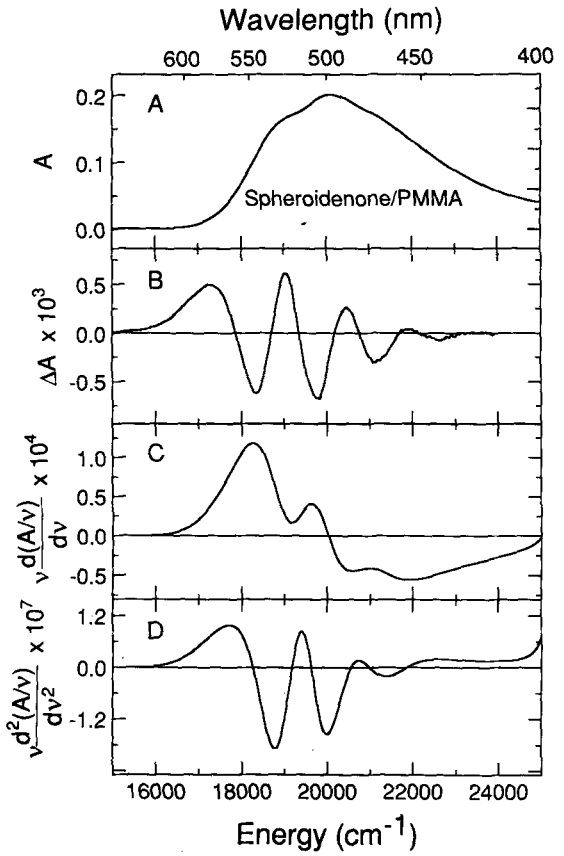

Fig. 8. (A) Absorption, (B) Stark effect, (C) first derivative and (D) second derivative of absorption spectra of pure all-*trans*-spheroidenone embedded in a PMMA film. $T = 77$ K, $\mathbf{F}_{ext} = 10^5$ V/cm and the ΔA spectrum is shown for $\chi = 54.7°$.

tural rearrangement. The first-derivative contribution is observable because $|\Delta\mu_A|$ is smaller for this complex. Based on the Stark effect spectrum it appears that all three carotenoids are equivalently affected by addition of detergent.

The Stark effect spectrum for spheroidene in RC complexes was investigated in wild-type strain 2.4.1 grown anaerobically (data not shown) and in carotenoidless strain R26 reconstituted with pure *trans*-spheroidene (Fig. 5). Both of these gave similar results; however, the analysis is more complex than for the B800-850 complex. Qualitatively, the magnitude of ΔA for comparable applied field strengths is substantially smaller in the RC complex than in the B800-850 complex. This is most easily seen by noting that the rather small Stark effect for the BChl monomer Q_x bands is at least evident in the RC spectrum on the same scale as ΔA for the carotenoid, whereas it is much smaller than the effect on the spheroidene bands in the B800-850 complex. It is also evident that the spheroidene absorption bands are considerably broader in the RC complex. Finally, the dependence of the ΔA spectrum on the experimental angle χ shown in Fig. 5B indicates that the electro-optic properties of the apparent vibronic components are not constant. These results are consistent with heterogeneity in the properties of the carotenoid binding site. The carotenoid in the RC binding site is known to be 15-15′-*cis* [20–22,30,31], although the X-ray structures all exhibit substantial disorder in the specific configuration of all the double bonds [20–22]. Interestingly, the RC appears to catalyze the isomerization of the carotenoid from all-*trans* to 15-15′-*cis*. Unfortunately, we do not have a good model molecule for the conformation in this binding site which could be studied in a simple nonpolar glass.

Analysis of spheroidenone Stark effect spectra

The lineshapes of the Stark spectra of spheroidenone in a 3MP glass, PMMA film, and in RCs are

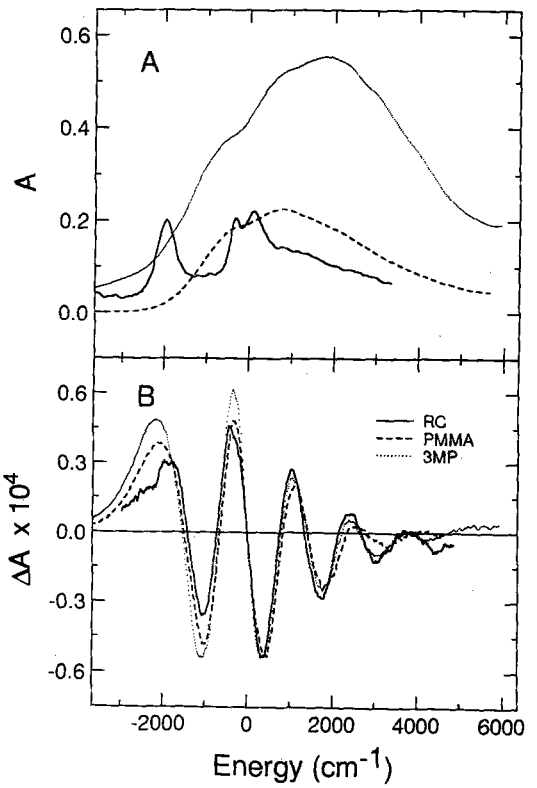

Fig. 9. Comparison of (A) absorption and (B) Stark effect spectra for semi-aerobically grown *Rb. sphaeroides* wild-type strain WS231 RCs containing spheroidenone, and pure spheroidenone in PMMA and 3-methylpentane matrices. $T = 77$ K, $\mathbf{F}_{ext} = 10^5$ V/cm, and the ΔA spectra are shown for $\chi = 54.7°$. The Stark effect spectra of the extracted chromophores were aligned with the red-side zero-crossing point of the first vibronic band of the Stark effect spectrum of the RC to facilitate comparison of the lineshapes. The spectra of spheroidenone taken in PMMA and in 3MP were shifted 701.9 and 419.5 cm^{-1} to the red, respectively. For the abscissa, the value of zero was assigned to $\nu = 18649$ cm^{-1} in the RC Stark effect spectrum. To facilitate comparison of lineshapes, the amplitude of the two Stark spectra for the extracted chromophores were adjusted to equal the magnitude of the minimum of the RC Stark effect spectrum at about 19000 cm^{-1}. The absorption spectra were then shifted and scaled accordingly (see text).

TABLE I

Values of electro-optic parameters $|\Delta\mu_A|$, ζ_A *and* $|Tr(\Delta\alpha)|$ *for spheroidene and spheroidenone in various matrices*

Chromophore/protein	Bulk matrix [a]	$\lvert\Delta\mu_A\rvert$ (D/f)	ζ_A (°)	$\lvert Tr(\Delta\alpha)\rvert$ [b] (Å^3/f^2)
Spheroidene				
B800-850, LDAO	glycerol	15.3±0.7	10±2	
B800-850, LDAO	PVA	13 ±3	≈0	
B800-850, LDS	PVA	6 ±1	<20	~1000
Rb. sphaeroides RC [c]	glycerol	3–8		
Pure *trans*-spheroidene	PMMA	<4.7	15±2	>500
Pure *trans*-spheroidene	3MP	<4.8	16±2	>700
Spheroidenone [d]				
B800-850, LDAO	glycerol	~35	≈10	
Various RC complexes [e]	glycerol	26–40	22±8	
Pure *trans*-spheroidenone				
origin	PMMA, 3MP	20 ± 2	18±4	
vibronic bands	PMMA, 3MP	20 ±10	<22	

[a] All data at 77 K.

[b] Although values of $|Tr(\Delta\alpha)|$ are not given for most of the samples, this does not imply that this component is small. Rather, the contribution from $\Delta\alpha$ is small compared to $|\Delta\mu_A|$, and therefore the ΔA spectral lineshape is not sensitive to it. We expect $\Delta\alpha$ to be similar for each carotenoid in different matrices (see text).

[c] *Rb. spheroides* R26 RCs reconstituted with pure spheroidene.

[d] The analysis of ΔA lineshapes for spheroidenone is complex as discussed in the text. The values given are approximate.

[e] The spheroidenone containing RCs investigated include: *Rb. sphaeroides* wild-type, R26 reconstituted with spheroidenone, and mutants (M)H202L (heterodimer) [35] and (L)H173L (reverse heterodimer) [44]; *Rb. capsulatus* wild type and (M)H200L heterodimer mutant [43].

remarkably similar. This is illustrated in Fig. 9B, where the positions of the ΔA spectra are aligned at the zero-crossing point on the low-energy side of the first vibronic band. Furthermore, it is evident that the spheroidenone contribution in the B800-850 complex (Fig. 2) is likewise very similar; it is not plotted in Fig. 9 because of the complication due to the presence of a significant amount of spheroidene. As seen in Fig. 9A, as well as in the spectra of various RCs (Fig. 6), the absorption spectra which give rise to these Stark effect spectra are very different, highlighting the difficulty in the data analysis, as well as in carotenoid bandshift or transient absorption measurements (see below). The similarity of the Stark effect spectra, particularly the width separating zero-crossing points, implies that the underlying field-sensitive component of the spheroidenone absorption in the RCs is not significantly different from that of the isolated chromophore.

Although it is straightforward to adjust the horizontal (cm^{-1}) scale to facilitate a comparison of the lineshapes, it is much more difficult to scale ΔA relative to A in a meaningful way. In the absence of clearly defined features in the absorption spectrum, this scaling offers the only approach to estimating the relative values of the electro-optic parameters from the Stark effect spectra. Therefore, we adopted a more indirect strategy, and begin by assuming that the ΔA lineshape is the result of contributions from the second derivative of A from the overlapping bands, i.e., we are assuming that the effect is due entirely to $|\Delta\mu_A|$. This seems reasonable given the very large magnitude of ΔA and the shape of the spectra, and assumes that a first-derivative component is dominated by the large second-derivative component. In Fig. 9B the Stark effect spectra for monomeric spheroidenone in both a glass and polymer matrix and in the *Rb. sphaeroides* wild-type RC were first scaled to the same field, and the differences in the magnitudes of the features in the three spectra were noted. The absolute magnitudes of the monomer Stark effect spectra were then adjusted to equal that of wild-type RCs, and the necessary corresponding scaling constants were applied to their absorption spectra. This analysis, depicted in Fig. 9, shows clearly that the amount of pure spheroidenone absorption required to give rise to the observed Stark effect spectrum is too large to be present in the RC absorption spectrum if $|\Delta\mu_A|$ were the same in pure spheroidenone as it is in the RC. In order to reproduce the magnitudes of the absorption and Stark effect spectra, $|\Delta\mu_A|$ of spheroidenone in the RC must be a factor of 1.3–2.0-times larger than that of the isolated chromophore.

Stark effect spectra in the Q_x region for a number of different RCs are compared in Fig. 6. It is evident that the dominant contribution is from the carotenoid in all cases. A recent report suggesting unusual Stark effects for the *Rb. capsulatus* heterodimer Q_x bands in this region of the spectrum [43] did not consider contributions from the carotenoids which we find to dominate the Stark spectrum completely. Furthermore, the

absorption spectra in Ref. 43 have been processed using an ill-defined baseline correction, leading to negative values of absorbance in the Q_x region which, of course, will lead to artifacts in the analysis. In general, great care must be taken to measure the zero of both A and ΔA in order to obtain a meaningful quantitative analysis.

In order to obtain a reasonable estimate for $|\Delta\mu_A|$ of spheroidenone in the B800-850 complex, we have used two approaches in analyzing the Stark effect data. Taking the value of ΔA of the peak minimum at 17575 cm^{-1} (Fig. 2) and the value of the second derivative for the most closely corresponding feature (shifted slightly to the blue due to overlap with the second-derivative feature from the BChl Q_x band), we calculate $|\Delta\mu_A| \approx 33\ D/f$ for the origin band. Alternatively, we can obtain an estimate for the second derivative of the origin band at 17575 cm^{-1} by using the ratio of 3:7 for the spheroidenone : spheroidene composition reported in Ref. 27. The second derivative was scaled at the peak of the spheroidene origin band (19400 cm^{-1}), while accounting for the different widths of the two Stark features and the proportion of the chromophore in the spectrum. This scaling is based on the approximation that the bands are Gaussians, in which case the ν-weighted second-dervative value at the peak of the band is inversely proportional to the square of the bandwidth (FWHM). Once the second derivative of the spheroidenone absorption band is obtained, it is used to calculate $|\Delta\mu_A| \approx 35\ D/f$ (for $\zeta_A = 10°$), which agrees closely with the value estimated by the more straightforward approach above. This value of $|\Delta\mu_A|$ is a factor of two larger than that obtained for spheroidene in the same complex and is more than 50% larger than that of extracted spheroidenone in a glassy matrix or polymer film. If this analysis is correct, then this is one of the largest changes in dipole moment observed for any molecule of which we are aware *.

It is not surprising that $|\Delta\mu_A|$ is larger for spheroidenone than spheroidene, given the structural differences between the two. The conjugated ketone in spheroidenone introduces significant electronic asymmetry for the π-electrons, which is not present for the more symmetric π-orbital system in spheroidene. It is likely that this leads to an increase in the inherent, permanent $\Delta\mu$, although a change in $\Delta\alpha$ may also occur [45]. The magnitude of the effect that the ketone has on the difference dipole for the extracted pigment is quite large, increasing the apparent $|\Delta\mu_A|$ 4-fold for spheroidenone relative to spheroidene when both are dissolved in PMMA.

The available data do not allow quantitative comparison of the effect of the conjugated ketone on $|\mathrm{Tr}(\Delta\alpha)|$, because the spheroidenone data could not be fit well by sums of derivatives. However, several qualitative inferences can be made. For spheroidene, $|\Delta\mu_A|$ remains roughly constant when transferred from a PMMA matrix to its binding site in the RC, but $|\Delta\mu_A|$ increases by about 50% when spheroidenone is transferred. These changes would result if $\Delta\alpha$ for spheroidenone were greater than that for spheroidene, and if the matrix electric field arising from the RC protein were greater than that from PMMA. A second observation which suggests a large $\Delta\alpha$ for spheroidenone is that its Stark effect features in the RC are significantly shifted to the red, relative to their position in PMMA. A much smaller shift is observed for spheroidene. The band shift is approx. 750 cm^{-1} to the red for spheroidenone, but only 190 cm^{-1} for spheroidene. These differences may simply reflect changes resulting from the *trans* to *cis* isomerization, but seem to indicate that the $\Delta\alpha$ accompanying the electronic transition of spheroidenone is probably greater than that for spheroidene.

As mentioned above, the case in which the Stark effect spectrum could be best modeled by a sum of derivatives of the absorption spectrum was spheroidene in the B800-850 complex. In most previously reported measurements, ΔA spectra were only obtained at discrete points and with considerably poorer signal to noise [34] than those obtained more recently at lower temperature. As a result, we have found many instances in which the ΔA lineshape cannot be fit in detail by a sum of derivatives, although, as in the present case, reasonable estimate can be obtained for the electro-optic parameters and useful comparisons can be made. The simplest source of discrepancy is that the spectral bands are inhomogenous with respect to the electro-optic parameters. Although distributions in parameter values could be used in the data analysis, this would likely increase the number of fitting parameters too much to be very useful. It is interesting to note that, in the example with the least anomalous absorption lineshape, spheroidene in the B800-850 complex, there appears to be the least amount of heterogeneity in the electro-optic parameters for the three carotenoids within the complex, as discussed above. Wortmann et al. [42] have performed spectral simulation calculations of the absorption and Stark effect spectra for the linear polyene 1,8-diphenyl-1,3,5,7-octatetraene in fluid cyclohexane at room temperature and have concluded that evidence exists for a heterogeneity of dipole moments and polarizabilities that precludes simple analysis of electro-optical spectra. This heterogeneity makes it impossible to distin-

* We note that this value of $|\Delta\mu_A|$ is substantially larger than observed for retinal in rhodopsin [33,40]. Furthermore, large nonlinear optical properties are likely to accompany this large value of $|\Delta\mu_A|$ (see for example Ref. 61).

guish accurately first-derivative (polarizability) and second-derivative (dipole moment) contributions. Finally, there may be cases in which the basic formulation of Liptay [39] may not be applicable. For example, in an analysis of recent Stark effect data on transition metal complexes [46], Reimers and Hush [41] have considered mechanisms by which the electro-optic properties can depend on the nuclear coordinate, which could then lead to unusual lineshapes in the Stark effect spectra. This behavior can exist in different vibronic bands coupled to the electronic transition, and even within one vibronic band due to the overlap of different homogeneous populations across the inhomogeneously broadened band. These considerations might be expected to have even larger consequences when the vibronic bands overlap, as is the case for the spheroidenone-containing samples studied in this work.

Carotenoid bandshift measurements

The observation that the spectra of carotenoids undergo shifts in response to changes in transmembrane potential and light-induced charge separation steps was first made in the mid-1950's [47,48]. Several research groups have used light, ionic gradients, and electric fields to introduce transmembrane potentials and then monitor the kinetics of spectral changes and measure the carotenoid difference spectra with the goal of determining a precise mechanism for the band shifts [49–52]. Schmidt and co-workers demonstrated that an applied electric field induced changes in the absorption spectra of several carotenoids in multilayers [53]. In the absence of direct information on $\Delta\boldsymbol{\mu}_A$, various indirect approaches were taken to determine the origin of the shift and to calibrate its response. One of the most important observations that has been made previously is that the band shift is approximately linear with respect to the apparent transmembrane potential [49,54,55].

In a native biological membrane, the carotenoid has a unique and fixed orientation with respect to the external field direction due to the transmembrane potential (the sample is uniaxially oriented with respect to the applied field). If $\Delta\boldsymbol{\mu}_A$ is responsible for the band shift, one predicts a linear field dependence and first derivative shape (band shift) because the change in transition energy is simply the product of the field with the projection of $\Delta\boldsymbol{\mu}_A$ on the field direction. Samples which are artificially oriented by insertion into a lipid bilayer or in a Langmuir-Blodgett film are often oriented biaxially, relative to the field direction due to a transmembrane potential. Hence, two populations with chromophore dipole moments having projections parallel and antiparallel to the field are present. So long as $\Delta\boldsymbol{\mu}_A \cdot \mathbf{F}_{int}$ (the Stark splitting) is comparable to or smaller than the inhomogeneous linewidth (nearly always the case), then ΔA should depend quadratically on the applied field and give a second derivative lineshape, if equal parallel and antiparallel orientational populations are present (Lockhart, D.J. and Boxer, S.G., unpublished results). An isotropic sample is just the extension to all possible parallel and antiparallel orientational populations. If $\Delta\boldsymbol{\alpha}$ is responsible for the band shift, the magnitude of the ΔA spectrum should be quadratic in the applied field, and have a first-derivative lineshape.

For our immobilized isotropic samples, all orientations of $\Delta\boldsymbol{\mu}_A$ are present relative to the externally applied field with the result that both shifts to higher and lower energy occur, and the Stark effect is expected and observed to be quadratic with field, despite the fact that the interaction between $\Delta\boldsymbol{\mu}_A$ and $\mathbf{F}_{ext}$ is identical to that for a uniaxially oriented sample. As stated above, the quadratic field dependence is expected for an isotropic sample whether $\Delta\boldsymbol{\mu}_A$ or $\Delta\boldsymbol{\alpha}$ is responsible for the effect; however, these origins are easily distinguished because they give different lineshape contributions to ΔA. In the early literature it was unclear whether the applied transmembrane potential actually translated into an equivalent field strength across the bilayer, and if contributions from $\Delta\boldsymbol{\mu}_A$, $\Delta\boldsymbol{\alpha}$, and changes in oscillator strength might conspire to give a linear field dependence [3].

Based on the results presented in this paper, it is clear that obtaining quantitative information from bandshift measurements on complex membranes containing more than one type of carotenoid or carotenoid-containing proteins which have different values of $\Delta\boldsymbol{\mu}_A$ can be a formidable task. In chromatophore membranes, which contain such a collection of different carotenoid-containing proteins, several groups have obtained data which implied the presence of multiple pools of carotenoid/protein complexes [52,56–58]. We are able to provide quite precise information on the electric field sensitivity of individual components, and, as is especially evident for the B800-850 complex, the carotenoid population within a single type of protein complex appears to be highly homogeneous. Using strains which selectively express antenna and/or RC proteins, it should be possible to obtain very accurate bandshift data.

The same issues arise for transient absorption measurements. When charge separation occurs in RCs, very large internal electric fields are generated due to the charges on the ions which are formed. Most of the early, detailed studies were performed on the carotenoidless *Rb. sphaeroides* R26 mutant, and interpretations of the bandshifts due to internal Stark effects, for example on the monomer BChl *a* band around 800 nm, are controversial and have not been evaluated quantitatively. Many recent studies involve RC mutants, generally grown semi-aerobically in order to minimize the pressure for reversion. Unfortunately,

the absorption spectrum of spheroidenone overlaps significantly with the Q_x bands of the monomer BChl and BPheo, a spectral region of critical importance in mechanistic studies. When transient absorption spectra are analyzed, it is typically assumed that internal Stark effects will produce simple band shifts, i.e., first-derivative shaped features in the transient absorption difference spectra. Underlying this expectation is the assumption that the Stark effect spectrum (ΔA due to an external applied field) is simply related to the absorption spectrum. This is the case for the monomer BChl *a* band around 800 nm, whose Stark effect spectrum is nearly exactly the second derivative of the absorption spectrum [4–7]. However, as seen in Stark effect spectra presented here, this is rarely the case for carotenoid bands, especially for spheroidenone. Because the absorption bands of spheroidenone are found to be highly sensitive to an applied electric field (as much as 10 times more than the monomer BChl *a* Q_y bands), large changes in absorption can be expected in this wavelength region upon charge separation; however, the shapes of the transient absorption difference spectra may not be simply the first derivative of the absorption, and features may be shifted quite far from the zero-field absorption maximum. Furthermore, the shapes of such transient absorption spectra should be very sensitive to the distribution of charge on the ions. Conversely, quantitative analysis of bandshifts may provide essential information on the charge distribution as a function of time during the charge separation process. It would be very useful to use host strains which are deficient in carotenoid biosynthesis such as the *Rb. sphaeroides* R26 strain, so that comparisons with and without carotenoid can be made, and so carotenoids such as spheroidene, whose spectra are simpler, can be reconstituted as a probe. In any event, quantitative evaluation of the electro-optic properties of carotenoid chromophores using Stark effect spectroscopy, provides the data needed for further analysis.

Acknowledgments

We thank Professor Harry Frank for his generosity in providing samples and advice which were indispensable to this work. We thank Professor Douglas Youvan for providing the strains of *Rb. capsulatus* used for preparation of pseudo wild-type and heterodimer RCs and Professor Craig Schenk for the strains of *Rb. sphaeroides* used for preparation of WS231, heterodimer, and reverse heterodimer RCs. This work was supported by a grant from the National Science Foundation Biophysics Program. M.A.S. is an MSTP trainee supported by grant GM07365 from NIGMS.

References

1 Goodwin, T. and Britton, G. (1988) in Plant Pigments (Goodwin, T.W., ed.), pp. 61–132, Academic Press, London.
2 Cogdell, R.J. and Frank, H.A. (1987) Biochim. Biophys. Acta 895, 63–79.
3 Wraight, C.A., Cogdell, R.J. and Chance, B. (1978) in The Photosynthetic Bacteria (Clayton, R.K. and Sistrom, W.R., eds.), pp. 471–511, Plenum, New York.
4 Lockhart, D.J. and Boxer, S.G. (1987) Biochemistry 26, 664–668; Biochemistry 26, 2958.
5 Lockhart, D.J. and Boxer, S.G. (1988) Proc. Natl. Acad. Sci. USA 85, 107–111.
6 Lösche, M., Feher, G. and Okamura, M.Y. (1987) Proc. Natl. Acad. Sci. USA 84, 7537–7541.
7 Lösche, M., Feher, G. and Okamura, M.Y. (1988) in The Photosynthetic Bacterial Reaction Center – Structure and Dynamics (Breton, J. and Vermeglio, A., eds.), pp. 151–164, Plenum, New York.
8 Lockhart, D.J. and Boxer, S.G. (1988) Chem. Phys. Lett. 144, 243–250.
9 Lockhart, D.J., Goldstein, R.F. and Boxer, S.G. (1988) J. Chem. Phys. 88, 1408–1415.
10 Gottfried, D.S., Stocker, J.W. and Boxer, S.G. (1991) Biochim. Biophys. Acta 1059, 63–75.
11 Gottfried, D.S., Steffen, M.A. and Boxer, S.G. (1991) Science 251, 662–665.
12 Cogdell, R.J. and Crofts, A.P. (1978) Biochim. Biophys. Acta 502, 409–416.
13 Evans, M.B., Cogdell, R.J. and Britton, G. (1988) Biochim. Biophys. Acta 935, 292–298.
14 Kramer, H.J.M., Van Grondelle, R., Hunter, C.N., Westerhuis, H.H.J. and Amesz, J. (1984) Biochim. Biophys. Acta 765, 156–165.
15 Trautman, J.K., Shreve, A.P., Violette, C.A., Frank, H.A., Owens, T.G. and Albrecht, A.C. (1990) Proc. Natl. Acad. Sci. USA 87, 215–219.
16 Allen, J.P., Theiler, R. and Feher, G. (1985) in Antennas and Reaction Centers of Photosynthetic Bacteria (Michel-Beyerle, M.E., ed.), pp. 82–84, Springer, Berlin.
17 Cogdell, R.J., Woolley, K., Mackenzie, R.C., Lindsay, J.G., Michael, H., Dobler, J. and Zinth, W. (1985) in Antennas and Reaction Centers of Photosynthetic Bacteria (Michel-Beyerle, M.E., ed.), pp. 85–87, Springer, Berlin.
18 Mantele, W., Steck, K., Wacker, T. and Welte, W. (1985) in Antennas and Reaction Centers of Photosynthetic Bacteria (Michel-Beyerle, M.E., ed.), pp. 89–91, Springer, Berlin.
19 Zuber, H. (1986) Trends Biochem. Sci. 11, 414–419.
20 Deisenhofer, J., Epp, O., Miki, K., Huber, R. and Michel, H. (1984) J. Mol. Biol. 180, 385–398.
21 Allen, J.P., Feher, G., Yeates, T.O., Komiya, H. and Rees, D.C. (1987) Proc. Natl. Acad. Sci. USA 84, 5730–5734 and 6162–6166.
22 Arnoux, B., Ducruix, A., Reiss-Husson, F., Lutz, M., Norris, J., Schiffer, M. and Chang, C.-H. (1989) FEBS Lett. 258, 47–50.
23 Takiff, L. and Boxer, S.G. (1988) J. Am. Chem. Soc. 110, 4425–4426.
24 Takiff, L. and Boxer, S.G. (1988) Biochim. Biophys. Acta 932, 325–334.
25 Schenck, C.C., Mathis, P. and Lutz, M. (1984) Photochem. Photobiol. 39, 407–417.
26 Frank, H.A. and Violette, C.A. (1989) Biochim. Biophys. Acta 976, 222–232.
27 Siefermann-Harms, D. (1985) Biochim. Biophys. Acta 811, 325–355.
28 Hayashi, H., Noguchi, T. and Tasumi, M. (1989) Photochem. Photobiol. 49, 337–343.
29 Breton, J. and Nabedryk, E. (1987) Topics Photosynth. 8, 159–195.

30 Chadwick, B.W. and Frank, H.A. (1986) Biochim. Biophys. Acta 851, 257–266.
31 Lutz, M., Szponarski, W., Berger, G., Robert, B. and Neumann, J.-M. (1987) Biochim. Biophys. Acta 894, 423–433.
32 Ponder, M. (1983) Ph.D. Thesis, Univeristy of California, Berkeley.
33 Ponder, M. and Mathies, R. (1983) J. Phys. Chem. 87, 5090–5098.
34 Liptay, W., Wortmann, R., Böhm, R. and Detzer, N. (1988) Chem. Phys. 120, 439–448.
35 Hammes, S.L., Mazzola, L., Boxer, S.G., Gaul, D.F. and Schenk, C.C. (1990) Proc. Natl. Acad. Sci. USA 87, 5682–5686.
36 Chadwick, B.W., Zhang, C., Cogdell, R.J. and Frank, H.A. (1987) Biochim. Biophys. Acta 893, 444–451.
37 Thayer, S.S. and Björkman, O. (1990) Photosyn. Res. 23, 331–343.
38 Myers, A. and Birge, R. (1981) J. Am. Chem. Soc. 103, 1881–1885.
39 Liptay, W. (1974) in Excited States (Lim, E.C., ed.), pp. 129–229, Academic Press, New York.
40 Mathies, R. and Stryer, L. (1976) Proc. Natl. Acad. Sci. USA 73, 2169–2173.
41 Reimers, J.R. and Hush, N.S. (1991) Proceedings of the NATO Conference on Theoretical Methods, Springer, Berlin, in press.
42 Wortmann, R., Elich, K. and Liptay, W. (1988) Chem. Phys. 124, 395–409.
43 DiMagno, T.J., Bylina, E.J., Angerhofer, A., Youvan, D.C. and Norris, J.R. (1990) Biochemistry 29, 899–907.
44 Schenk, C.C., Gaul, D., Steffen, M., Boxer, S.G., McDowell, L., Kirmaier, C. and Holten, D. (1990) Series in Biophysics, Springer, Berlin, in press.
45 Reich, R. and Sewe, K. (1977) Photochem. Photobiol. 26, 11–17.
46 Oh, D.H. and Boxer, S.G. (1990) J. Am. Chem. Soc. 112, 8161–2.
47 Chance, B. and Smith, L. (1955) Nature (London) 175, 803–806.
48 Chance, B. (1958) Brookhaven Symp. Biol. 11, 74–86.
49 Jackson, J.B. and Crofts, A.R. (1969) FEBS Lett. 4, 185–189.
50 Reich, R., Scheerer, R., Sewe, K.-U. and Witt, H.T. (1976) Biochim. Biophys. Acta 449, 285–294.
51 De Grooth, B.G. and Amesz, J. (1977) Biochim. Biophys. Acta 462, 237–246.
52 De Grooth, B.G., Van Gorkum, H.J. and Meiburg, R.F. (1980) Biochim. Biophys. Acta 589, 299–314.
53 Schmidt, S., Reich, R. and Witt, H.T. (1971) Naturwissenschaften 58, 414.
54 Junge, W. and Jackson, J.B. (1982) in Photosynthesis, Vol. 1, Energy Conversion in Plants and Bacteria (Govindjee, ed.), pp. 589–646, Academic Press, New York.
55 Crielaard, W., Hellingwerf, K.J. and Konings, W.N. (1988) Biochim. Biophys. Acta 973, 205–211.
56 De Grooth, B.G. and Amesz, J. (1977) Biochim. Biophys. Acta 462, 247–258.
57 Symons, M., Swysen, C. and Sybesma, C. (1977) Biochim. Biophys. Acta 462, 706–717.
58 Symons, M. and Crofts, A. (1980) Z. Naturforsch. 35c, 139–144.
59 Boxer, S.G., Goldstein, R.A., Lockhart, D.J., Middendorf, T.R. and Takiff, L. (1989) J. Phys. Chem. 93, 8280–8294.
60 Mazzola, L.T., Middendorf, T.R., Boxer, S.B., Gaul, D. and Schenck, C. (1991) Biophys. J. 59, 139a.
61 Huang, J., Lewis, A. and Raising, Th. (1988) J. Phys. Chem. 92, 1756–1759.
62 Middendorf, T.R. (1991) Ph.D. Thesis, Stanford University.